



## Organic Bioelectronics for Neural Interfaces

Journal:	<i>Journal of Materials Chemistry C</i>
Manuscript ID:	TC-HIG-02-2015-000569.R1
Article Type:	Highlight
Date Submitted by the Author:	18-May-2015
Complete List of Authors:	Fang, Yan; Tianjin Polytechnic University, School of Mechanical Engineering and Automatization Li, Xinming; National Center for Nanoscience & Technology, China, Fang, Ying; National Center for Nanoscience & Technology, China,

## Organic Bioelectronics for Neural Interfaces

By Yan Fang,<sup>a</sup> Xinming Li,<sup>b,\*</sup> and Ying Fang,<sup>b, c,\*</sup>

<sup>a</sup>School of Mechanical Engineering and Automatization, Tianjin Polytechnic University, Tianjin 300160, China

<sup>b</sup>CAS Key Laboratory for Biomedical Effects of Nanomaterials & Nanosafety, National Center for Nanoscience and Technology, 11 Beiyitiao Street, Beijing 100190, China;

<sup>c</sup>CAS Center for Excellence in Brain Science, 320 Yue Yang Road, Shanghai 200031, China;

E-mail: [fangy@nanoctr.cn](mailto:fangy@nanoctr.cn), [lixm2@nanoctr.cn](mailto:lixm2@nanoctr.cn)

Keywords: conducting polymer, organic bioelectronics, electrochemical transistor, neural interfaces, flexible electronics

Organic bioelectronics offers important opportunities to study complex biological systems, such as neural networks, and develop new biomedical tools for the diagnosis and treatment of brain disease. This Highlight is focused on recent progress in neural recording and stimulation enabled by using conducting polymers as active elements in bioelectronics, with an emphasis on the underlying mechanisms for the improved signal transduction capabilities at organic/neural interfaces. These studies are classified into two categories, electrochemical electrodes and electrochemical transistors, according to their operating principles. Future challenges and directions at organic/neural interfaces are discussed as a conclusion.

### 1. Introduction

The brain consists of billions of neurons that are interconnected into a complex neural network. Communication in the neural network is achieved when bioelectrical signals, called action potentials (APs), are generated and propagated across synapses between adjacent neurons. The brain processes information through spatiotemporal activity

patterns of neural networks, thus a comprehensive analysis of neural activity is central to understand brain functions and also diagnose brain diseases.<sup>[1]</sup> Various technologies have been developed to study neural activity at different space and time scales. Imaging techniques, such as functional magnetic resonance imaging (fMRI) and positron-emission tomography (PET), allow three-dimensional localization of active regions by measuring hemodynamic changes in the functioning brain.<sup>[2]</sup> Despite the non-invasive nature of fMRI and PET, both techniques suffer from low spatial and temporal resolution, and the relationship between the measured hemodynamic signals and the underlying neural activity is indirect. The US Brain Research through Advancing Innovative Neurotechnologies (BRAIN) Initiative and the EU Human Brain Project (HBP) both emphasize on the development of innovative technologies that can record and analyze the activity of large sets of neurons at high spatiotemporal resolution.<sup>[3]</sup> The approaches that show the most promise for high spatiotemporal mapping of neural activity are optical and electrical methods. Optical techniques based on calcium or voltage-sensitive dyes have become a powerful tool for highly parallel recording of neural activity.<sup>[4,5]</sup> However, it remains challenging for optical approaches to access deep brain activity due to the fundamental imaging-depth limit. Furthermore, the sampling speed of optical techniques is currently limited by fluorescent reporter dyes.<sup>[5]</sup> Bioelectronics is complementary to optical techniques in that it can access deep brain structures and allow label-free detection of neural activity at high temporal resolution.

Bioelectronics directly communicates with neuronal systems via electronic elements that transduce electric signals to and from bioelectric signals of neurons. Traditional metal electrodes are capable of probing and stimulating neural activity at single-cell level with high temporal resolution. Moreover, metal microelectrode arrays (MEAs) can simultaneously monitor the activity of a large number of neurons.<sup>[6]</sup> Over the past decades, electrical recording by metal-based bioelectronics has significantly contributed to our basic understanding of neural activity. Today, implantation of stimulating electrodes into the brain is increasingly explored for treatment of neurological disorders, such as Parkinson's disease.<sup>[7]</sup>

Bioelectronics currently faces two major challenges for neural interfaces. First, metals conduct electrons and neuronal systems carry ionic signals, therefore the quality of recorded and injected signals by bioelectronics is largely determined by the coupling between electrons and ions at metal/neural interfaces.<sup>[6]</sup> Thermal noise, also known as Johnson noise, arises from the electrode-electrolyte impedance at metal/neural interfaces, which leads to relatively poor signal-to-noise (SNR) of metal electrodes. Second, the hard and dry metal surfaces are quite distant from the soft and wet neural tissues, which complicates the long-term stability of metal/neural interfaces.<sup>[8]</sup> Specifically, commonly used metal electrodes and MEAs are made of stiff materials, such as platinum and silicon, with elastic moduli from 10 to 100 GPa, which significantly exceeds those of neural tissues in the range of kPa to MPa. The drastic mechanical mismatch between implanted electrodes and neural tissues results in relative micromotion of electrodes within tissues. Micromotion causes inflammatory

response of the neural tissues. This chronic inflammation results in the formation of glial scars that insulate the electrodes from neural signals, which eventually leads to electrode failure in long-term studies.<sup>[9]</sup>

Ideal neural interfaces should enable effective and reliable signal transduction between neurons and electronic materials. Indeed, recent progress in bioelectronics has been driven by advances in material research, especially organic electroactive materials. Specifically, organic bioelectronics based on conducting polymers (CPs) has been shown to provide more effective transduction interfaces to neurons than metals, thus enhancing both neural recording and stimulation characteristics of organic bioelectronics.<sup>[10-14]</sup> Furthermore, organic bioelectronics is particularly promising to improve the long-term success of implanted neural interfaces due to their mechanical flexibility and biocompatibility.<sup>[15, 16]</sup>

This Highlight is focused on recent progress in organic bioelectronics interfaced to neuronal systems. These studies are classified into two categories: (i) organic electrochemical electrodes and (ii) organic electrochemical transistors, according to their signal transduction mechanisms. For each category, we critically evaluate the specific properties of organic bioelectronics that fulfill essential requirements of neural interfaces. Finally, challenges towards the implementation of organic bioelectronics are identified, and future promising research directions are discussed.

## **2. Conducting Polymers and their Organic Electronics**

CPs combine the electrical properties of semiconductors and metals with the mechanical flexibility of plastics. Since the discovery of CPs in 1977,<sup>[17]</sup> the field of

organic electronics has experienced an enormous development. An important frontier of this field is at the interface with biology.<sup>[15, 18-20]</sup> In particular, CPs provide a variety of advantages over metals and inorganic semiconductors at neural interfaces, including the ease of synthesis and modification, low-temperature and cost-effective processing, and the compatibility with flexible plastic substrates.<sup>[21-23]</sup> The “soft” nature of CPs and their chemical similarities to biomolecules promote their tight integration with neuronal systems, allowing effective communication between neural and electronic signals. Recently, organic electronics based on poly(3,4-ethylenedioxythiophene) (PEDOT), poly(pyrrole) (PPy), and their derivatives have received tremendous attention for neural recording and stimulation.<sup>[10, 11]</sup>

Electrochemical polymerization has been widely applied to deposit thin CP films with well-defined structures, and the electrical properties of the CP films can be facily modified by chemical doping during deposition. For example, PEDOT doped with poly(styrenesulfonate) (PEDOT:PSS) is one of the most commonly used composite CPs.<sup>[24-26]</sup> PEDOT:PSS is a p-type semiconductor in which a negative sulfonate group on the PSS chain creates a hole carrier on the PEDOT (Figure 1).<sup>[27, 28]</sup> Under application of a bias voltage, the hole carrier moves along the  $\pi$ -conjugated PEDOT backbone while the negative sulfonate group remains immobile. Among CPs, PEDOT:PSS has shown the highest conductivity (up to 1000 S/cm) and good chemical stability in aqueous solution. In addition, ions from the electrolyte solution can penetrate the bulk of the PEDOT:PSS film to directly modulate its doping level.

The ability of PEDOT:PSS to conduct ions opens up a new communication channel with bionic signals. It has been reported that the ionic conductivity in PEDOT:PSS is close to that of the bulk electrolyte.<sup>[29]</sup> The combined high ionic and electronic conductivities makes PEDOT:PSS one of the most attractive candidates for neural interfaces.

### 3. Organic Bioelectronics for Neural Interfaces

#### 3.1. Neural recording and stimulation

We firstly describe the working principles of neural recording by traditional metal electrodes and inorganic transistors. Figure 2a and 2b depict the equivalent circuits at the neuron-metal and neuron-transistor interface, respectively.<sup>[30]</sup> During an AP of a neuron, ionic currents flow across the cell membrane, which changes both the intracellular potential,  $V_M$ , and extracellular potential,  $V_J$ . The extracellular potential then leads to an electrochemical current at the metal-electrolyte interface (Figure 2a) or modulates the Fermi level of the semiconductor (Figure 2b).

In the brain, the summed bioelectric currents from multiple neurons within a small volume superimpose at a given location and generate a local potential. Historically, this local potential has been referred to as the electrocorticography (ECoG) when recorded by grid electrodes placed on the cortical surface, or as the single-unit activity (SUA) and local field potential (LFP) when recorded by a small intracortical electrode inserted deep into the brain.<sup>[1]</sup> The amplitude of the extracellular potential scales inversely with the distance from the spiking neuron. As a result, the larger the distance of the recording electrode from the source, the less informative the measured

signal becomes about the underlying neurological processes. Therefore, intracortical electrodes yield the most informative signals containing both fast spiking activities and slow oscillations. Over the past decades, CP-coating has been extensively applied to improve both the electrical characteristics and biocompatibility of intracortical electrodes. On the other hand, ECoG is less invasive than penetrating intracortical electrodes and can record over a large area of the cortical surface. ECoG has become a critical tool for studying cortical phenomena in clinical settings, and the spatial resolution of ECoG has been substantially improved by using flexible, organic bioelectronics, which is discussed in details in the next section.

Neural stimulation by metal electrodes is a primary method to repair or restore neurological functions.<sup>[31]</sup> The charge movements at electrode/neural interfaces during stimulation are reversed compared with recording. For stimulation, charges are delivered by the electrodes to neurons, which is characterized by the charge injection capacity (CIC) at electrode/neural interfaces. The amount of charges required for neural stimulation is orders of magnitude higher than signals recorded by the electrodes, mainly due to ineffective coupling at electrode/neural interfaces. In addition, it is desirable that the stimulation electrodes are small enough to enable selective stimulation of a targeted neuron population. However, high current density on small electrodes can cause both undesirable electrochemical reactions on the electrodes and inflammatory response of tissues.<sup>[16]</sup> A viable approach to reduce the injection currents is to improve the charge injection efficiency at electrode/neural interfaces. Therefore the improved coupling at electrode/neural interfaces is a critical

for both neural recording and stimulation, in which organic electroactive materials have become an attractive candidate.<sup>[32]</sup>

### 3.2. Neural recording and stimulation with organic electrochemical electrodes

Figure 2a depicts the equivalent circuit for a metal electrodes in extracellular recording. The extracellular potential,  $V_J$ , induces an electric current at the metal surface through the electrochemical impedance,  $Z_e$ , at metal/electrolyte interface.

The sensitivity of the metal electrode is determined by SNR. At low frequency region ( $< 10\text{kHz}$ ) where neural recording is performed, thermal noise at metal/electrolyte interface dominates and is given by  $\overline{\delta V_J^2} = 4k_B T \times \text{Re}\{Z_e\} \times \Delta f$ , where  $\text{Re}\{Z_e\}$  is the resistive component of  $Z_e$  and  $\Delta f$  is the frequency bandwidth. Since  $Z_e$  scales inversely with the area of the electrode,  $A$ , we have the relationship of

$\sqrt{\overline{\delta V_J^2}} \propto \frac{1}{\sqrt{A}}$ , indicating that the noise is inversely proportional to the square root of

the electrode area. Thus, an immense amount of effort has been made to increase the effective area of the metal electrodes to achieve better SNR for neural recording.

Surface coating of electroactive PPy:PSS and PEDOT:PSS has been shown to greatly increase the effective area of the electrode and reduce the impedance. Martin *et al.* (2001)<sup>[10]</sup> demonstrated the earliest example of organic electrochemical electrodes by electrochemically depositing PPy:PSS onto gold electrodes. The thickness of the PPy:PSS film can be precisely controlled during electrochemical deposition. It was found that the roughness of the PPy:PSS film increased with thickness and played an important role in interfacial impedance. An optimum PPy:PSS film thickness of 13

$\mu\text{m}$  resulted in the lowest impedance that is 26 times lower than the bare gold electrodes.

Stability of the electrodes is a prerequisite in chronic, long-term neural recording. PPy is unstable and can be easily oxidized or decomposed in aqueous solutions. On the other hand, PEDOT has a dioxyethylene bridging group across the 3- and 4-positions of the hetero-ring, which blocks the possibility of coupling and leads to superior electrochemical stability in aqueous solutions. Martin *et al.* (2003)<sup>[11]</sup> electrochemically deposited PEDOT:PSS films on gold electrodes (Figure 3a). It was found that the PEDOT:PSS coating has a fuzzy film morphology which allows fast ion transport across the film. As a result, the impedance was decreased by almost two orders of magnitude compared to bare gold electrodes (Figure 3b). In addition, PEDOT:PSS films demonstrated a significant improvement in electrochemical stability than PPy:PSS (Figure 3c).

Another advantage of electrochemical deposition method is that it can be applied to deposit CPs together with bioactive molecules onto neural electrodes. In particular, nona-peptide CDPGYIGSR has been shown to promote cell adhesion and neuron extension. Martin *et al.* (2003)<sup>[11]</sup> further co-deposited nona-peptide CDPGYIGSR with PEDOT:PSS onto Au electrodes. It was found that the PEDOT:PSS /DCDPGYIGSR coating successfully promoted neuron attachment and growth. Importantly, intracortical electrodes coated with PEDOT:PSS /DCDPGYIGS enabled high quality acute recording from guinea pig cerebellum (Figure 3d).

Flexible implantable electrodes are of great importance to form neural interfaces with high biocompatibility and stability. Very recently, Buzsaki *et al.* (2015)<sup>[14]</sup> developed a thin and ultraconformable neural interface array, the NeuroGrid, for the recording of ECoG signals (Figure 4a). The total thickness of the parylene C substrates is only 4  $\mu\text{m}$ , and thin PEDOT:PSS films were electrochemically deposited on  $10 \times 10 \mu\text{m}^2$  gold electrodes to substantially decrease the electrochemical impedance. The mechanical flexibility of the NeuroGrid allows it to closely follow the cortical surface topography of rats and human patients, leading to tight coupling between electrodes and neuronal tissues (Figure 4b). As a result, NeuroGrid recorded both LFPs and APs from superficial cortical neurons with high SNR (Figure 4d). In addition, the NeuroGrid is easily scalable to cover large surface areas of the brain with high fidelity, which opens up new opportunities to study neural network.

Stimulation neural electrodes have been widely used to improve or restore main functions of nervous systems for patients with neural damage. There has been tremendous effort to develop stimulation electrodes with low interfacial impedance and high charge storage capacity. In particular, CPs have demonstrated significant potentials in neural stimulation. Otto *et al.* (2009)<sup>[33]</sup> compared the performances of PEDOT-coated electrodes with bare iridium oxide ( $\text{IrO}_x$ ) electrodes. PEDOT-coated electrodes exhibit enhanced charge storage capacity of  $75.6 \pm 5.4 \text{ mC/cm}^2$  compared to  $28.8 \pm 0.3 \text{ mC/cm}^2$  of  $\text{IrO}_x$ . During repetitive pulsing, PEDOT-coated electrodes demonstrated stable electrical characteristics, even at high current densities which cause  $\text{IrO}_x$  instability. Green *et al.* (2013)<sup>[16]</sup> assessed the charge injection limit and

long-term stability of PEDOT-coated electrode arrays under stimulation in biologically relevant electrolytes. The PEDOT films showed high structural and electrical stability following ethylene oxide sterilization and under stimulation in physiological saline. The charge injection limit of PEDOT-coated electrodes was found to be 30 times larger in physiological saline and 20 times larger in protein supplemented media than bare platinum electrodes. In addition, in vivo studies showed that PEDOT-coated electrodes had low potential excursions, and electrically evoked potentials could be detected within the visual cortex.

### 3.3. Neural recording with organic electrochemical transistors

A transistor has three terminals: source, drain, and gate. The equivalent circuit of a p-channel transistor is shown in Figure 2b, where  $V_g$  is gate voltage,  $V_d$  is drain voltage,  $I_d$  is the drain current, and  $C_g$  is the gate capacitance. A transistor can work both as a detector and an amplifier in that it allows a small input voltage,  $V_g$ , to control a large output current,  $I_d$ . The output drain current is related to the input gate voltage by the transconductance as  $g_m = \frac{\partial I_d}{\partial V_g}$ , thus  $g_m$  represents the amplification gain of the transistor. In the linear operation region of a transistor, we have

$g_m = \frac{\mu C_g V_d}{L^2}$ , where  $\mu$  is the carrier mobility and  $L$  is the channel length of the semiconductor.

In neural recording, the extracellular potential acts as a gate voltage input that modulates the output current of the transistor. The most important merit of using a transistor to record neural signals is that it provides signal amplification directly at the

recording sites, thus reducing noise interference from the transmission line and external circuitry. Fromherz *et al.* (1991)<sup>[34]</sup> reported the earliest example to record neural signals by using electrolyte–oxide–silicon field-effect transistors (EOS-FETs) (Figure 5a). The gate capacitance,  $C_g$ , of the EOS-FETs consists of an electrolyte double-layer capacitance,  $C_{dl}$ , in series with an oxide capacitance,  $C_{ox}$ . Since the double-layer capacitance is much larger than the oxide capacitance, the total gate capacitance is dominated by the oxide capacitance which is inversely proportional to the thickness of silicon dioxide layer. As a result, the amplification gain of the transistor decreases with the oxide thickness.

One advantage of organic transistors is that they are oxide-free, and the organic semiconductor channels are in direct contact with the electrolyte. The gate capacitance of organic semiconductors is determined by the double-layer capacitance which is commonly orders of magnitude higher than the oxide capacitance of inorganic semiconductors (Figure 5b). In addition, the porous structures of organic films further increase their gate capacitance by increasing the effective gate areas, leading to large transconductance and amplification gain of the organic electrochemical transistors. Malliaras *et al.* (2013)<sup>[27]</sup> reported that PEDOT:PSS based organic electrochemical transistors showed a peak  $g_m = 402 \text{ S} \cdot \text{m}^{-1}$  at  $V_d = -0.6 \text{ V}$  in 100 mM NaCl solutions (Figure 5c&d), which exceeds inorganic transistors based on silicon, zinc oxide, and graphene.

A unique feature of organic semiconductors is their ability to conduct both electrons and ions. Ions from the electrolyte can penetrate the bulk of the polymer and directly

dope the semiconductor channel, which thus effectively modulates the carrier density and consequently the drain current of the transistor. Malliaras *et al.* (2013)<sup>[29]</sup> studied the ion mobility in thin PEDOT:PSS films. The 400 nm-thick PEDOT:PSS film was found to be highly hydrated, which leads to the formation of water channels occupying most of the film volume. As a result, PEDOT:PSS films can transport small ions efficiently through the water channels. The ion drift mobilities measured at electrolyte/PEDOT:PSS junctions were comparable to the bulk electrolyte.

The combined high electronic and ionic mobilities of PEDOT:PSS transistors are of particular importance for neural interfaces. Malliaras *et al.* (2013)<sup>[12]</sup> reported a highly flexible ECoG device based on PEDOT:PSS-based electrochemical transistors (Figure 6a). The PEDOT:PSS transistors were embedded in ultrathin parylene film of 4  $\mu\text{m}$  thick, and each ECoG device consists of 17 transistors with a channel length of 6  $\mu\text{m}$  and width of 15  $\mu\text{m}$ . It was shown that the ECoG device formed highly conformable interfaces with the somatosensory cortex surface of rats (Figure 6b). Significantly, compared with PEDOT:PSS-coated electrochemical electrodes, the PEDOT:PSS-based electrochemical transistors displayed superior SNR for *in vivo* neural recording due to local signal amplification and noise reduction (Figure 6c). The high sensitivity and mechanical flexibility of PEDOT:PSS-based electrochemical transistors make them a promising candidate in neuroscience.

#### **4. Summary: Challenges and Opportunities**

There is an urgent need for new tools to study neural networks and to treat neural disorders. Organic bioelectronics is a rapidly growing field which offers tremendous

opportunities for neural interfaces. Although considerable progress has been made at organic/neural interfaces, numerous challenges remain. These include: (i) the carrier mobility of organic semiconductors is still orders of magnitude lower than inorganic semiconductors. For example, the mobility of hole carriers in PEDOT:PSS is usually around  $1 \text{ cm}^2/\text{V.s}^{[35]}$ , whereas inorganic semiconductors such as III-IV group<sup>[36]</sup> and graphene<sup>[37, 38]</sup> show high carrier mobility up to  $10^4 \text{ cm}^2/\text{V.s}$ . The low mobility values of organic semiconductors compromise the amplification gain of the neural signals; (ii) the understanding of the noise in organic electrochemical transistors is very limited. Noise in electrolyte-gated inorganic transistors has been extensively studied. It was shown that inorganic semiconductors are not limited by the thermal noise. Instead,  $1/f$  noise, or flicker noise, is dominant in inorganic semiconductors at low-frequency region.<sup>[39, 40]</sup> However, there still lacks a detailed study on the noise characteristics in organic electrochemical transistors;<sup>[41, 42]</sup> (ii) chronic evaluation of organic/neural interfaces is lacking. Although *in vivo* acute studies have shown that flexible organic bioelectronics offers highly sensitive recording of neural signals, long-term chronic evaluation of organic/neural interfaces is urgently needed for the development of implantable devices.

To conclude, ideal neural interfaces are characterized by the following desired attributes: high recording sensitivity, high charge injection capacity, and long-term stability. Owing to the chemical similarity and compatibility between organic electroactive materials and neuronal systems, the benefits of using organic electronics for neural interfaces are obvious. It will be especially important for future studies to

translate these laboratory works into clinical applications, such as neural prosthesis.

Finally, the development of integrated and multifunctional organic bioelectronics will be of great importance for both fundamental and clinical neuroscience.

### Acknowledgements

This work was supported by the National Natural Science Foundation of China (21322302 and 21173055), the National Basic Research Program of China (973 Program) (2011CB932700).

### References

- [1] G. Buzsáki, C. A. Anastassiou and C. Koch, *Nature Review in Neuroscience*, 2012, **13**, 407-420.
- [2] R. Peyron, B. Laurent and L. García-Larrea, *Neurophysiologie Clinique/Clinical Neurophysiology*, 2000, **30**, 263-288.
- [3] A. P. Alivisatos, A. M. Andrews, E. S. Boyden, M. Chun, G. M. Church, K. Deisseroth, J. P. Donoghue, S. E. Fraser, J. Lippincott-Schwartz, L. L. Looger, S. Masmanidis, P. L. McEuen, A. V. Nurmikko, H. Park, D. S. Peterka, C. Reid, M. L. Roukes, A. Scherer, M. Schnitzer, T. J. Sejnowski, K. L. Shepard, D. Tsao, G. Turrigiano, P. S. Weiss, C. Xu, R. Yuste and X. Zhuang, *ACS Nano*, 2013, **7**, 1850-1866.
- [4] L. B. Cohen, B. M. Salzberg and A. Grinvald, *Annual Review in Neuroscience*, 1978, **1**, 171-182.
- [5] S. A. Kim and S. B. Jun, *Experimental Neurobiology*, 2013, **22**, 158-166.
- [6] M. E. Spira and A. Hai, *Nature Nanotechnology*, 2013, **8**, 83-94.
- [7] S. Hemm and K. Wårdell, *Medical & Biological Engineering & Computing*, 2010, **48**, 611-624.
- [8] N. A. Kotov, J. O. Winter, I. P. Clements, E. Jan, B. P. Timko, S. Campidelli, S. Pathak, A. Mazzatenta, C. M. Lieber, M. Prato, R. V. Bellamkonda, G. A. Silva, N. W. S. Kam, F. Patolsky and L. Ballerini, *Advanced Materials*, 2009, **21**, 3970-4004.
- [9] C. A. Chestek, V. Gilja, P. Nuyujukian, J. D. Foster, J. M. Fan, M. T. Kaufman, M. M. Churchland, Z. Rivera-Alvidrez, J. P. Cunningham, S. I. Ryu and K. V. Shenoy, *Journal of Neural Engineering*, 2011, **8**, 045005.
- [10] X. Cui, J. F. Hetke, J. A. Wiler, D. J. Anderson and D. C. Martin, *Sensors and Actuators A: Physical*, 2001, **93**, 8-18.
- [11] X. Cui and D. C. Martin, *Sensors and Actuators B: Chemical*, 2003, **89**, 92-102.
- [12] D. Khodagholy, T. Doublet, P. Quilichini, M. Gurfinkel, P. Leleux, A. Ghestem, E. Ismailova, T. Hervé, S. Sanaur, C. Bernard and G. G. Malliaras, *Nature Communications*, 2013, **4**, 1575.
- [13] V. Benfenati, S. Toffanin, S. Bonetti, G. Turatti, A. Pistone, M. Chiappalone,

- A. Sagnella, A. Stefani, G. Generali, G. Ruani, D. Saguatti, R. Zamboni and M. Muccini, *Nature Materials*, 2013, **12**, 672-680.
- [14] D. Khodagholy, J. N. Gelinias, T. Thesen, W. Doyle, O. Devinsky, G. G. Malliaras and G. Buzsaki, *Nature Neuroscience*, 2015, **18**, 310-315.
- [15] M. Berggren and A. Richter-Dahlfors, *Advanced Materials*, 2007, **19**, 3201-3213.
- [16] R. A. Green, P. B. Matteucci, R. T. Hassarati, B. Giraud, C. W. D. Dodds, S. Chen, P. J. Byrnes-Preston, G. J. Suaning, L. A. Poole-Warren and N. H. Lovell, *Journal of Neural Engineering*, 2013, **10**.
- [17] H. Shirakawa, E. J. Louis, A. G. MacDiarmid, C. K. Chiang and A. J. Heeger, *Journal of the Chemical Society, Chemical Communications*, 1977, 578-580.
- [18] J. Rivnay, R. M. Owens and G. G. Malliaras, *Chemistry of Materials*, 2014, **26**, 679-685.
- [19] G. Tarabella, F. Mahvash Mohammadi, N. Coppede, F. Barbero, S. Iannotta, C. Santato and F. Cicoira, *Chemical Science*, 2013, **4**, 1395-1409.
- [20] M. Muskovich and C. J. Bettinger, *Advanced Healthcare Materials*, 2012, **1**, 248-266.
- [21] J. Smith, R. Hamilton, I. McCulloch, N. Stingelin-Stutzmann, M. Heeney, D. D. C. Bradley and T. D. Anthopoulos, *Journal of Materials Chemistry*, 2010, **20**, 2562-2574.
- [22] L. Basiricò, P. Cosseddu, B. Fraboni and A. Bonfiglio, *Thin Solid Films*, 2011, **520**, 1291-1294.
- [23] S. Ouyang, Y. Xie, D. Wang, D. Zhu, X. Xu, T. Tan and H. H. Fong, *Journal of Nanomaterials*, 2015, 603148.
- [24] W. Brütting, *Physics of Organic Semiconductors*, John Wiley & Sons, 2006.
- [25] J. Yang and D. C. Martin, *Sensors and Actuators B: Chemical*, 2004, **101**, 133-142.
- [26] U. A. Aregueta-Robles, A. J. Woolley, L. A. Poole-Warren, N. H. Lovell and R. A. Green, *Frontiers in Neuroengineering*, 2014, **7**, 15.
- [27] D. Khodagholy, J. Rivnay, M. Sessolo, M. Gurfinkel, P. Leleux, L. H. Jimison, E. Stavrinidou, T. Herve, S. Sanaur, R. M. Owens and G. G. Malliaras, *Nature Communications*, 2013, **4**, 2133.
- [28] M. Nikolou and G. G. Malliaras, *The Chemical Record*, 2008, **8**, 13-22.
- [29] E. Stavrinidou, P. Leleux, H. Rajaona, D. Khodagholy, J. Rivnay, M. Lindau, S. Sanaur and G. G. Malliaras, *Advanced Materials*, 2013, **25**, 4488-4493.
- [30] L. Yang, Y. Li and Y. Fang, *Advanced Materials*, 2013, **25**, 3881-3887.
- [31] S. F. Cogan, in *Annual Review of Biomedical Engineering*, Annual Reviews, Palo Alto, 2008.
- [32] R. A. Green, N. H. Lovell, G. G. Wallace and L. A. Poole-Warren, *Biomaterials*, 2008, **29**, 3393-3399.
- [33] S. J. Wilks, S. M. Richardson-Burns, J. L. Hendricks, D. C. Martin and K. J. Otto, *Frontiers in Neuroengineering*, 2009, **2**, 7.
- [34] P. Fromherz, A. Offenhausser, T. Vetter and J. Weis, *Science*, 1991, **252**, 1290-1293.

- [35] Q. Wei, M. Mukaida, Y. Naitoh and T. Ishida, *Advanced Materials*, 2013, **25**, 2831-2836.
- [36] M. Shur, B. Gelmont and M. Asif Khan, *Journal of Electronic Materials*, 1996, **25**, 777-785.
- [37] K. I. Bolotin, K. J. Sikes, Z. Jiang, M. Klima, G. Fudenberg, J. Hone, P. Kim and H. L. Stormer, *Solid State Communications*, 2008, **146**, 351-355.
- [38] E. Shi, H. Li, L. Yang, J. Hou, Y. Li, L. Li, A. Cao and Y. Fang, *Advanced Materials*, 2015, **27**, 682-688.
- [39] P. Dutta and P. M. Horn, *Reviews of Modern Physics*, 1981, **53**, 497-516.
- [40] Z. Cheng, J. Hou, Q. Zhou, T. Li, H. Li, L. Yang, K. Jiang, C. Wang, Y. Li and Y. Fang, *Nano Letters*, 2013, **13**, 2902-2907.
- [41] P. V. Necliudov, S. L. Rumyantsev, M. S. Shur, D. J. Gundlach and T. N. Jackson, *Journal of Applied Physics*, 2000, **88**, 5395-5399.
- [42] L. Ke, S. B. Dolmanan, L. Shen, C. Vijila, S. J. Chua, R.-Q. Png, P.-J. Chia, L.-L. Chua and P. K.-H. Ho, *Journal of Applied Physics*, 2008, **104**, 124502.

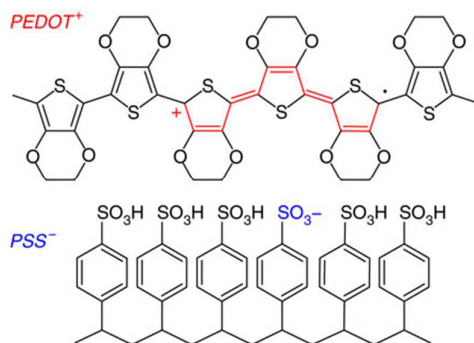


**Figure 1.** Chemical structure of PEDOT and PSS. A hole carrier (red) is compensated by a sulphonate ion (blue) on the PSS chain. Modified from reference 27 with permission from the Nature Publishing Group.

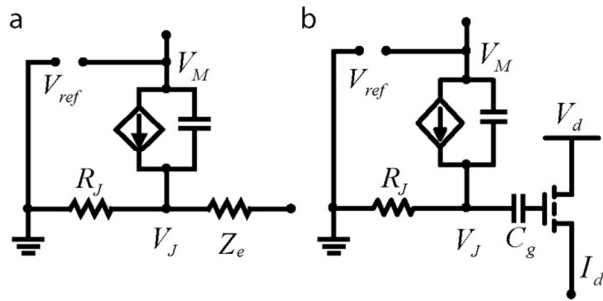


**Figure 2.** Equivalent circuits for extracellular recording with a metal electrode (a) and a transistor (b).

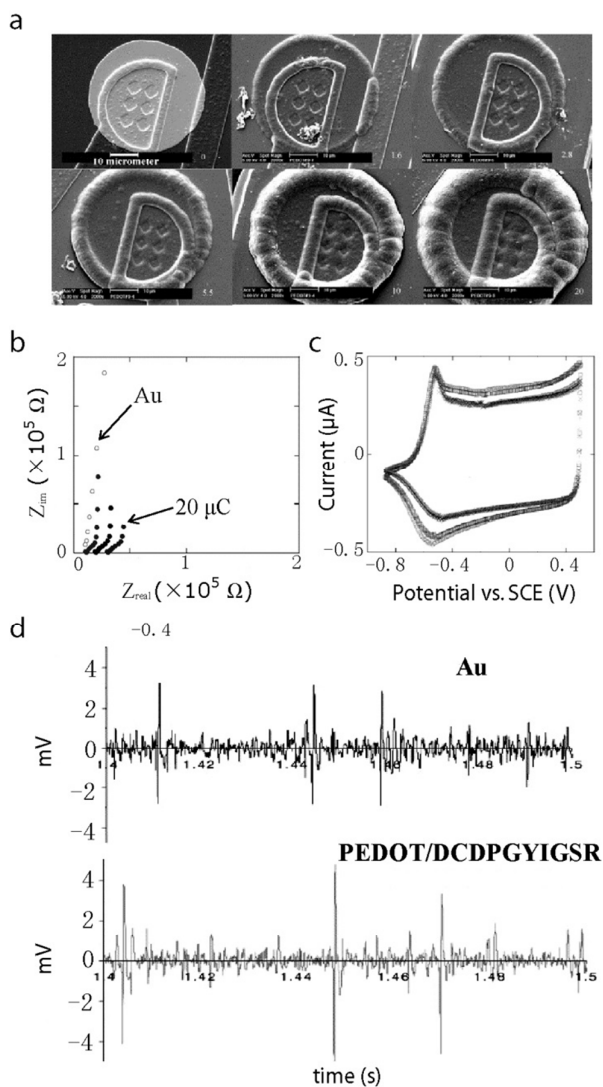


**Figure 3.** (a) Galvanostatic growth of PEDOT:PSS on gold electrodes. The deposition charges are 0, 1.6, 2.8, 5.5, 10, and 20  $\mu\text{C}$ , respectively; (b) Impedance spectroscopy of PEDOT/PSS deposited on the gold electrode (with deposition charge of 5, 10 and 20  $\mu\text{C}$  from left to right) in comparison with the bare gold electrode. (c) High electrochemical stability of PEDOT:PSS after 400 cycles. Scan rate 0.1 V/s; (d) In vivo acute recording from guinea pig cerebellum with PEDOT:PSS/DCDPGYIGSR coated electrode in comparison to bare electrode. Modified from reference 11 with permission from the Elsevier Science B.V..

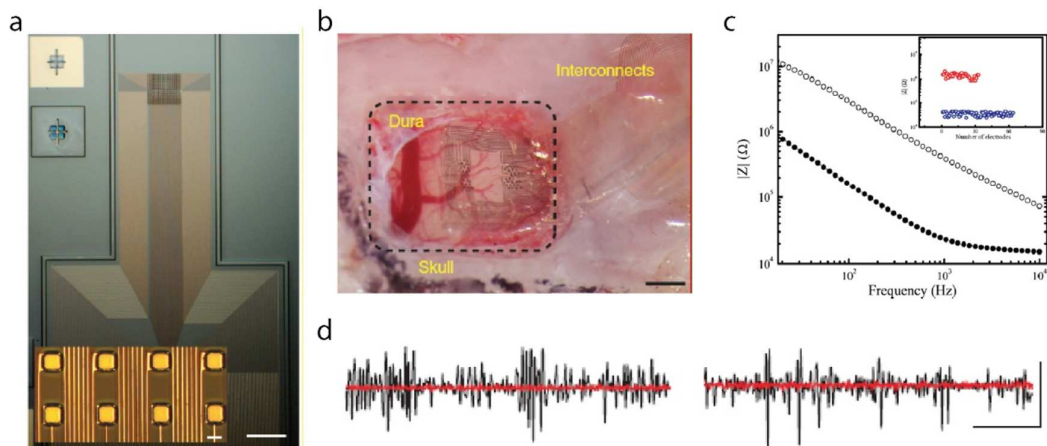


**Figure 4.** (a) Optical image of a 256-channel NeuroGrid. Inset, PEDOT:PSS coated gold electrodes. Scale bars, 1 mm and 10 μm (inset); (b) A NeuroGrid conforms to the surface of the rat somatosensory cortex. Scale bar, 1 mm; (c) Comparison of impedance between NeuroGrid (filled circles) and bare gold electrodes (open circles); (d) High-pass-filtered (500 Hz) time traces recorded in a freely moving rat from the surface of cortex (left) and hippocampus (right). Modified from reference 14 with permission from the Nature Publishing Group.

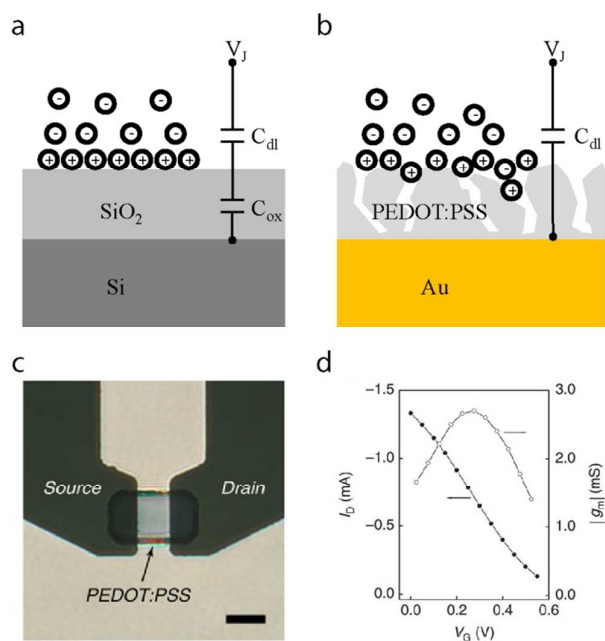


**Figure 5.** (a) Schematic of an electrolyte–oxide–silicon transistor; (b) Schematic of an electrolyte-gated PEDOT:PSS electrochemical transistor; (c) Optical image of a PEDOT:PSS transistor. Scale bar, 10  $\mu\text{m}$ ; (d) Transfer curve and the associated transconductance of a PEDOT:PSS transistor in 100 mM NaCl solutions. Modified from reference 27 with permission from the Nature Publishing Group.

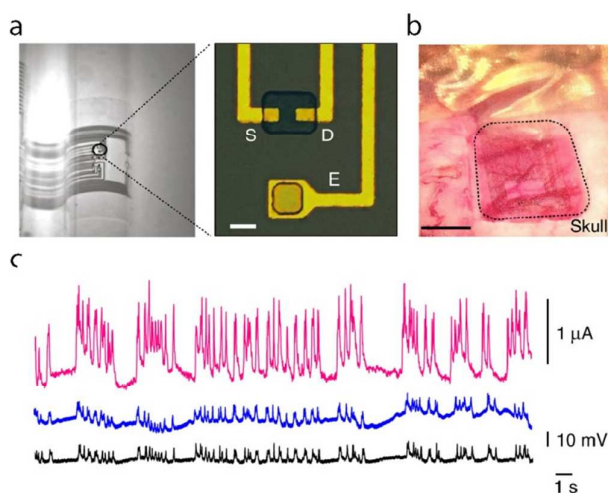


**Figure 6.** (a) Optical images of a flexible ECoG device conforming onto a curvilinear surface (left) and the channels of a PEDOT:PSS transistor and a PEDOT:PSS electrode (right). Scale bar, 10  $\mu\text{m}$ ; (b) Optical image of a flexible ECoG device placed on the somatosensory cortex of a rat. Scale bar, 1 mm; (c) Neural recordings from a PEDOT:PSS transistor (pink), a PEDOT:PSS electrode (blue), and an Ir-penetrating electrode (black). The transistor was biased at  $-0.4\text{V}$  with the gate voltage of  $0.3\text{ V}$ . Modified from reference 12 with permission from the Nature Publishing Group.





38x40mm (299 x 299 DPI)